GEOLOGICA CARPATHICA, JUNE 2014, 65, 3, 241–253 doi: 10.2478/geoca-2014-0014

Mineralogical, geochemical and micromorphological evaluation of the Plio-Quaternary paleosols and calcretes from Karahamzalı, Ankara (Central Turkey)

CEREN KÜÇÜKUYSAL[1]✉ and SELIM KAPUR[2]

[1]General Directorate of MTA, Geological Research Departement, Building G, Room: 204, 06800 Çankaya, Ankara, Turkey; ✉kucukuysal09@yahoo.com.tr
[2]Çukurova University, Department of Soil Science, 01330 Balcalı, Adana, Turkey; kapurs@cu.edu.tr

(Manuscript received September 13, 2013; accepted in revised form March 11, 2014)

Abstract: We present the mineralogical, micromorphological, and geochemical characteristics of the paleosols and their carbonates from Karahamzalı, Ankara (Central Turkey). The paleosols include calcretes of powdery to nodular forms and alternate with channel deposits. The presence of pedofeatures, such as clay cutans, floating grains, circumgranular cracks, MnO linings, secondary carbonate rims, traces of past bioturbation and remnants of root fragments are all the evidence of pedogenesis. Bw is the most common soil horizon showing subangular-angular blocky to granular or prismatic microstructures. Calcretes, on the other hand, are evaluated as semi-mature massive, nodular, tubular or powdery forms. The probable faunal and floral passages may also imply the traces of life from when these alluvial deposits were soil. The presence of early diagenetic palygorskite and dolomite together with high salinization, high calcification and low chemical index of alteration values are evidence of the formation of calcretes under arid and dry conditions. $\delta^{13}C$ compositions of the carbonates ranging from –7.11 ‰ to –7.74 ‰ VPDB are comformable with the world pedogenic carbonates favouring the C4 vegetation; likely $\delta^{18}O$ compositions of the carbonates are between –3.97 ‰ and –4.91 ‰ which are compatible with the paleosols formed under the influence of meteroic water in the vadose zone.

Key words: Calcrete, paleosol, Central Anatolia, Plio-Quaternary, stable isotope, Aridity.

Introduction

Paleosols from fluvio-lacustrine settings in Central Anatolia are still unknown. What we know about them is limited to some contributions from Atabey et al. (1998), Küçükuysal (2011), Küçükuysal et al. (2012). However, much more attention was devoted to the Mediterranean paleosols around Adana and Mersin in the south of Turkey. Paleosols and related calcretes are widespread throughout Turkey, for example, in Southern Anatolia in Adana (Kapur et al. 1987, 1990, 1993, 2000; Atalay 1996), in Mersin (Eren 2007; Eren et al. 2008; Kadir & Eren 2008; Eren & Hatıpoğlu-Bağcı 2010; Eren 2011) and in Central Anatolia in Kırşehir (Atabey et al. 1998; Gürel & Kadir 2006, 2008) in Cappadocia and in Ankara (Küçükuysal 2011 and Küçükuysal et al. 2012). The age of the calcretes in Southern Anatolia was determined by ESR and TL (Özer et al. 1989; Atalay 1996) and in Central Anatolia by ESR (Küçükuysal et al. 2011).

Paleosols have been thought to be very complex structures, but they are actually just soils formed on a landscape of the past (Kraus 1999). According to the paleopedological point of view of Retallack (2001), soil has a definition of a material forming the surface of a planet or similar body and altered in place from its parent material by physical, chemical or biological processes. Due to their structures and properties, as Morozova (1995) summarized, paleosols provide complex information about (i) soil processes shaping the soil profile itself during pedogenesis in the warm interglacials and interstadials, (ii) natural processes which characterize the transition to cold semicycles (glacial stages) and (iii) diagenetic processes. Therefore, paleosols and paleosol carbonates are widely used as sources of evidence for paleoclimatology studies. Paleosol carbonates — the calcretes or caliches — are very important materials for interpreting especially the semi-arid to arid climatic conditions of the past (James 1972; Goudie 1973, 1983; Tucker 1991). This study uses the definition of calcretes defined by Wright & Tucker (1991) that calcrete is a near surface, terrestrial accumulation of predominantly calcium carbonate, which occurs in a variety of forms from powdery to nodular to highly indurated, resulting from the cementation and displacive/replacive introduction of calcium carbonate into soil profiles, bedrock and sediments in areas where vadose and shallow phreatic groundwaters become saturated with respect to calcium carbonate. The mineralogical and chemical composition of pedogenic phyllosilicates, which form in a soil through alteration of detrital clays or by primary precipitation, are strongly controlled by the chemical activity of the soil solution, which in turn is influenced by the amount and seasonality of rainfall (Buol et al. 1997; Tabor 2002). This relationship clearly manifests the sensitivity of clay minerals to the climatic conditions at the time of formation. The geochemical characteristics of the paleosols and their carbonates are clearly important proxies revealing the climatic history of the soil. The recent studies on paleosol geochemistry (Nesbitt & Young 1982; Maynard 1992; Retallack 1997, 2001; Sheldon & Tabor 2009) stated that different proxies based on geochemical analyses can be used to infer the pedogenic processes revealing the effect of chemical weathering in paleosols.

The study area is in the south of Ankara around Karahamzalı village. The paleosol section with calcretes of low- to medium maturity begins to be visible around Lake Mogan towards Kulu, Konya. All the way along the Konya road, red coloured paleosols with calcretes could be recorded. Therefore, the areal distribution of this paleosol continues towards the southern part of Ankara. Towards southern Turkey, paleosols become more reddish with calcretes of medium- to high maturity level. These paleosols from the southern part are well-studied, and this points to a strong need for such studies of Central Anatolian paleosols.

The purpose of this study is (i) to explain the field characteristics of Plio-Quaternary paleosols and calcretes in Karahamzalı, Central Anatolia, (ii) to reveal their mineralogical compositions with their micromorphological properties defining the Pedogenic and diagenetic features and (iii) to present oxygen and carbon isotope analysis of the carbonates to emphasize their potential to reconstruct the climatic conditions during the Plio-Pleistocene in the region. In this respect, we employed mineralogical, micromorphological, geochemical and stable isotopic proxies all together to define the characteristics of the paleosols and also to evaluate the Plio-Quaternary paleoclimates in Central Anatolia.

Materials and methods

The Karahamzalı site in Ankara was selected as the most appropriate setting to study paleosol development for obtaining high resolution and reliable proxy data. The paleosols were investigated on the basis of colour changes and mottling revealing the horizon developments. The calcrete morphologies and the contact relationships between calcretes and the paleosols were also recorded during the field studies. 22 samples from paleosols and their carbonates (calcretes) were collected from the newly exposed fresh surfaces of ourcrops/road cuts and also by means of drilling operations. The drilling operation for Karahamzalı section was accomplished from the ground to a depth of 27 m. The soil colours were determined by the Munsell Colour Scale in the field under moist conditions. The thin sections of the Karahamzalı samples were prepared according to Retallack (2001) and Fitzpatrick (1993) at the Thin Section Preparation Laboratory in the Department of Geology at the University of Western Ontario, Canada. 15 appropriate samples were selected and analysed for their palinological compositions by Dr. Zühtü Batı. The mineralogical analysis was conducted by the X-Ray Diffraction equipment at the Department of Earth Sciences in the University of Western Ontario and Scanning Electron Microscope at the Central Laboratory, Middle East Technical University. Randomly-oriented powdered samples and the clay-fraction samples were mounted on glass slides and scanned using a Rigaku diffractometer (45 mA, 160 kV), equipped with Co-Kα radiation. Randomly-oriented samples were scanned from 2° to 42° 2Θ, using a step size of 0.02° 2Θ, and a scan rate of 10° 2Θ/min; and air-dried and ethylene glycol solvated samples were scanned from 2° to 32° 2Θ, using a step size of 0.01° 2Θ, and a scan rate of 1° 2Θ/min. Combined procedures of Thorez (1976), Jackson (1979), Brindley & Brown (1980), Tucker (1988) and Moore & Reynolds (1989), were followed during the preparation of the randomly-oriented powder and the saturated slides (for the clay minerals) for x-ray diffraction. Ca, K and Mg-saturated and glycerol solvated slides were prepared for each soil clay-size sample and x-rayed at room temperature, whereas the K-saturated samples were also x-rayed after heating to 300 °C and 500 °C. Isotope analysis ($\delta^{13}C$ and $\delta^{18}O$ analyses of the carbonates) was performed at the Laboratory for Stable Isotope Science in the Department of Earth Sciences at the University of Western Ontario. A multiprep device coupled to a VG Optima dual inlet stable isotope ratio mass spectrometer was used for this procedure. For the determinations of the geochemical compositions of the paleosols and their carbonates, the ICP-AES technique was employed by ACME Laboratories, Canada. The soil properties under the microscope were all defined in the Soil Laboratories of the Soil Science Department of the Çukurova University. Selected Au-Pd high vacuum coated samples were studied under the scanning electron microscope in the Central Laboratory of the Middle East Technical University by a QUANTA 400F Field Emission Scanning Electron Microscope at 1.2 nm resolution. The Energy Dispersive X-ray Spectrometer (EDX) was also employed to obtain the chemical analysis of the specific locations on the undisturbed samples.

Geological setting, paleosol/calcrete description and the depositional environment

The study area is located in the southwest of Ankara, near the Karahamzalı village (39°16′30.56″ N and 32°57′30.70″ E) (Fig. 1A). The geology of the area was obtained by the field studies conducted by Akçay et al. (2008). The stratigraphic section drawn in this study combines both this study and the field descriptions of this paper. The geological map of the study area is given in Fig. 1B. The oldest unit is the Dizilitaşlar Formation of the Paleocene–Early Eocene, which is composed of turbiditic conglomerate, sandstone, claystone and resifal limestone blocks. The Çayraz Formation of the Middle Eocene unconformably overlies the Dizilitaşlar Formation. It was deposited as conglomerate and sandstone in shallow marine and deep marine environments of turbiditic conglomerate-limestones. Conformable above, the İncik Formation was deposited as an alternation of evaporitic, continental conglomerate, sandstone, mudstone at the bottom and gypsum-anhydrite and mudstone at the middle, cross-laminated conglomerate and sandstones at the top. The evaporitic unit of this formation is called the Sekili evaporate member. The age of the formation is Late Eocene–Oligocene. The Central Anatolian Group, which has a widespread occurrence in the region, was unconformably overlain by the Late Eocene–Oligocene units. This formation consists of conglomerate, sandstone, mudstone, gypsum, anhydrite and limestone — ignimbrite intercalations. It is a continental unit of Middle Miocene-Pliocene age. The coeval İnsuyu

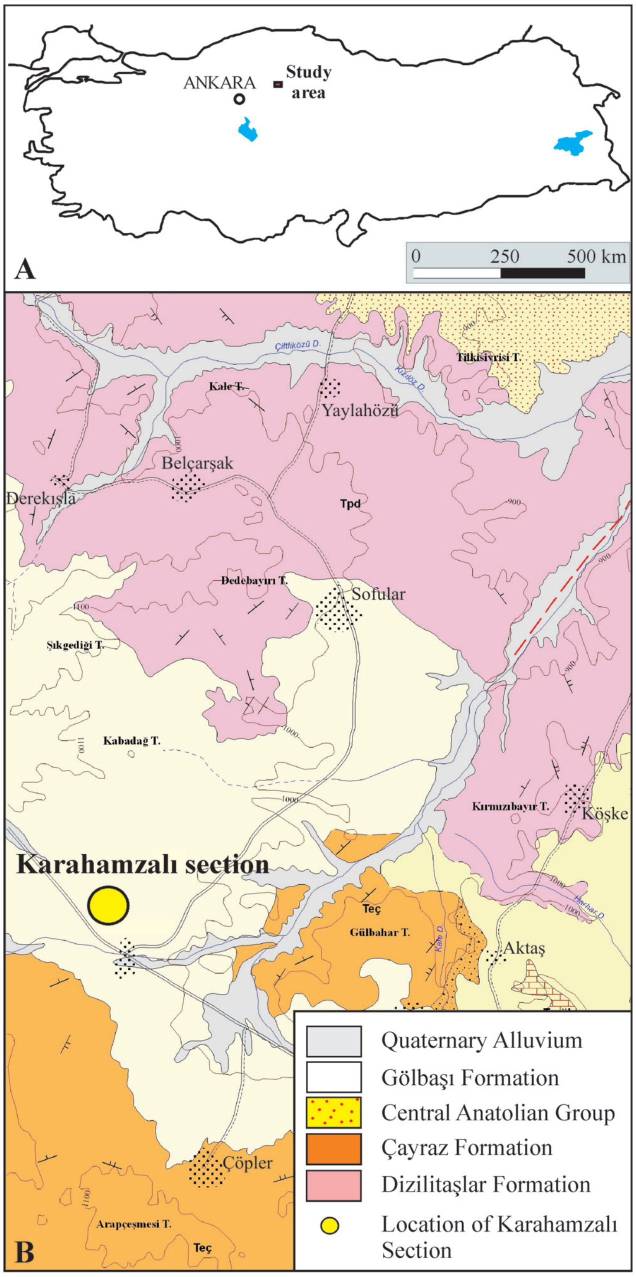

Fig. 1. A — Map of Turkey showing the location of Ankara and Karahamzalı; **B** — Geological map of the study area representing the positions and the ages of the lithological units and the location of the Karahamzalı section (Dönmez et al. 2008).

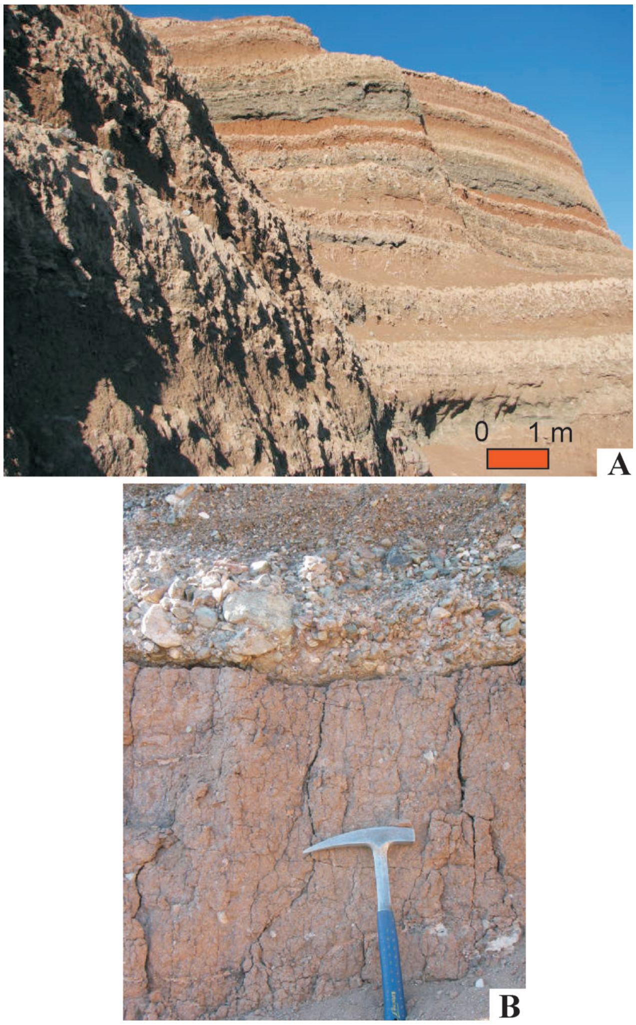

Fig. 2. A — Field view of the studied section in which red coloured alluvial deposits together with calcrete formations alternating the channel conglomerates; **B** — Field view of the paleosols with sharp upper contacts with the channel deposits (the hammer is 33 cm long).

Formation was a product of a lacustrine environment where carbonate deposition was high. The Kozaklı Limestone Member was deposited as lacustrine limestone of the Late Miocene age. The Gölbaşı Formation of Pliocene age unconformably overlies the Miocene units and is formed from alluvial fan and fluvial deposits. The youngest units in the study area are the Quaternary alluvium deposits (Fig. 1B).

The road cut located in the Karahamzalı village is the sampling site of this study (Fig. 2A). The studied section which is 39 m deep is in the continental rock units of the Gölbaşı Formation which is composed of grey, red and brown coloured, unconsolidated, poly-origin conglomerate, sandstone and mudstone. The soil features (e.g. soil horizons, soil structures and traces of biological activity) of the reddish brown mudrocks are the attributes designating the paleosols with calcretes. Küçükuysal (2011) stated that the presence of pedofeatures, such as clay cutans, floating grains, circumgranular cracks, MnO linings, secondary carbonate rims, traces of past bioturbation and remnants of root fragments clarify that the studied reddish alluvial deposits are paleosols and the carbonate concretions are their calcretes. The paleosol layers have sharp upper contacts with the overlying channel deposits (Fig. 2B). The calcretes are massive, nodular, tubular and powdery in form and show downward transitional gradations (Fig. 2A). In total a 39 m succession is recorded in the study area (Fig. 3). Red-brownish coloured fine grained mudstones with carbonate accumulations alternate with channel deposits.

The columnar section defines the stratigraphic relation of the lithologies with their field observations, soil morphologies and Munsell Colours (Fig. 3). The lowermost unit is the

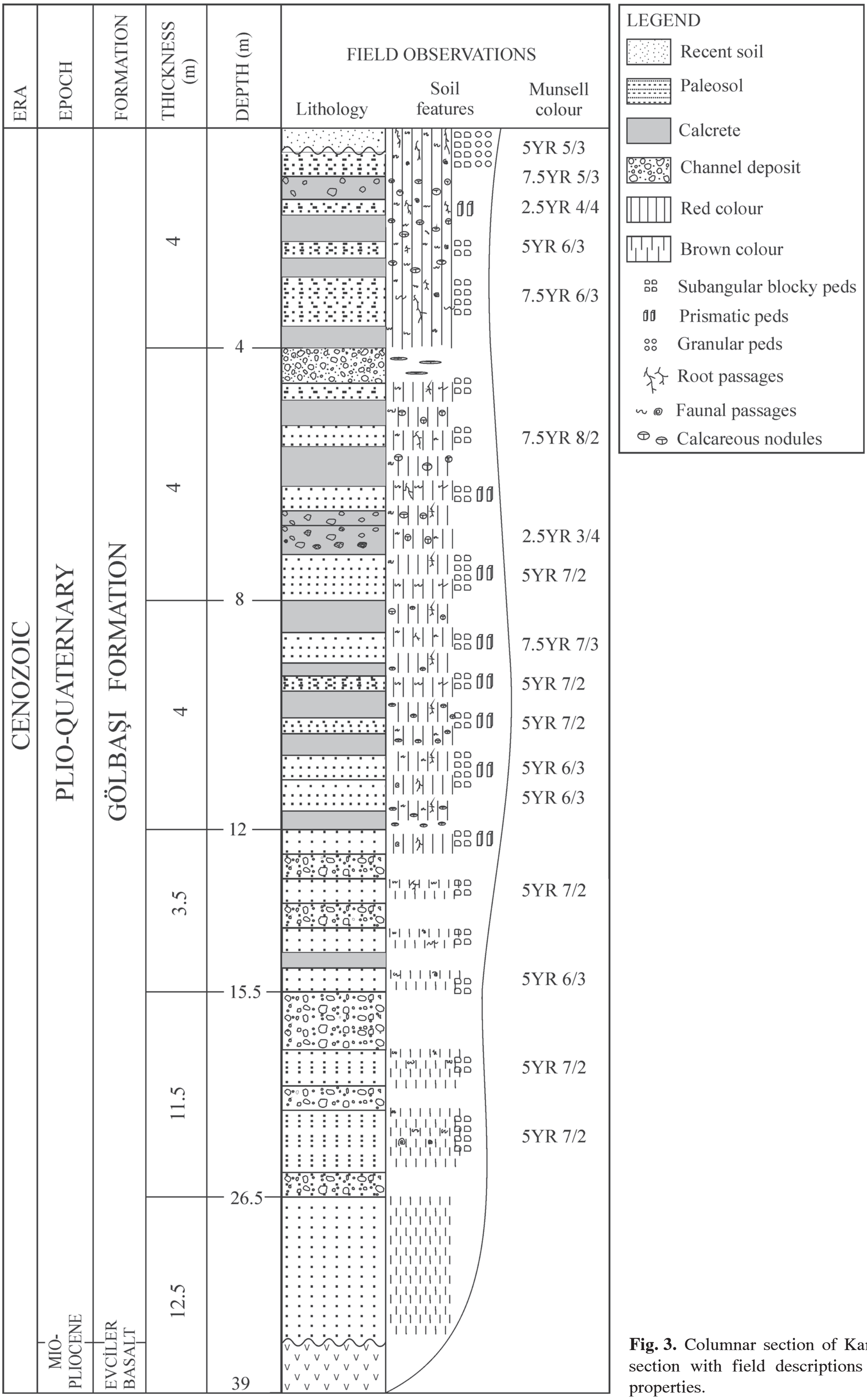

Fig. 3. Columnar section of Karahamzalı section with field descriptions and soil properties.

Mio-Pliocene Evciler Basalt (Dönmez et al. 2008), where unconformably above this unit, brownish red coloured mudstones/paleosols alternate with channel deposits up to 4 m depth. However, the paleosols are divided into 3 separate groups in terms of their macrostructures through the section. The first group from bottom to 13 m depth has almost only subangular blocky ped structure with a relatively low amount of faunal and floral passages. The recorded Munsell colours of the units within this range are 5YR 7/2 and 5YR 6/3. Calcretes have sharp upper contact and transitional lower contact with the old soils. Their poorly developed profiles include calcretes varying from powdery to nodular (Fig. 3). From 13 m to 4 m depth, the second group of paleosols was determined with both subangular blocky and prismatic ped structures. They become more reddish relative to the lower levels and still show alternation with channel deposits (Fig. 3). This group of paleosols has more faunal and floral passages with respect to the lower paleosols but illustrates the same contact features. The Munsell colours observed within this range for paleosols and their carbonates are 7.5YR 8/2, 2.5YR 3/4, 5YR 7/2, 7.5YR 7/3 and 5YR 6/3. At the top of the section, paleosols become more reddish in colour with subangular blocky, prismatic and also granular structural units. Faunal and floral passages are the largest within this range. The Munsell colours recorded area 5YR 5/3, 7.5YR 5/3, 2.5YR 4/4, 5YR 6/3, 7.5YR 6/3 (Fig. 3). The youngest unit is the recent soil deposit observed with red colour and high carbonate accumulation. The age of the calcretes in this succession was interpreted as Plio-Quaternary based on the stratigraphic position of the paleosols and the comparative age of the underlying volcanic unit together with the stratigraphically coeval paleosols in Bala, where the calcretes were dated as Middle Pleistocene (Küçükuysal et al. 2011) (Fig. 3).

Results

Mineralogy

Almost all of the paleosol samples contained quartz and feldspar as the detrital non-clay component. However, calcite and dolomite are oppositely present. Non-clay minerals (quartz, feldspar, calcite and dolomite) were identified within a size fraction of less than 63 μm. Quartz was determined by the presence of 2 prominent peaks at 4.27 Å and 3.34 Å. Feldspars, however, were determined by the most intense peak at 3.2 Å. Calcite was determined with a sharp and intense peak at 3.03 Å and dolomite with 2.89 Å. According to the peak intensities of the minerals on the XRD diagrams of the Karahamzalı section, the relative amounts of the non-clay minerals and the total amount of clay minerals within the bulk composition were calculated according to the method of Gündoğdu (1982) (Table 1). According to this method, the intensity factors of 0.35, 0.74, 1.62, 1 and 14.63 were used for quartz (3.34 Å), calcite (3.04 Å), feldspar (3.18–3.20 Å), dolomite (2.89 Å) and total clay minerals (4.53 Å), respectively. Quartz is present throughout the section, but it shows a decreasing trend towards the upper part of the section and reaches almost a constant value close to the upper levels. Its abundance varies

Table 1: Semi-quantitative analysis of bulk composition of samples from the Karahamzalı section.

Sample	Quartz	Calcite	Feldspar	Dolomite	Clay	Total
U13	4.1	0.0	0.0	52.3	43.6	100.00
U12	11.9	0.0	0.0	0.0	88.1	100.00
U11	8.5	0.0	0.0	0.0	91.5	100.00
U10	2.6	1.7	0.0	66.3	29.4	100.00
U8	6.4	2.2	0.0	4.1	87.3	100.00
U7	3.0	0.0	0.0	46.9	50.1	100.00
U6C	3.9	0.0	0.0	49.1	47.0	100.00
U6S	6.6	0.0	5.8	0.0	87.6	100.00
U5	6.1	0.0	5.2	29.8	59.0	100.00
U4	6.2	0.0	11.2	19.5	63.0	100.00
U3	9.5	0.0	5.5	0.0	85.0	100.00
U2	5.2	0.0	0.0	33.2	61.5	100.00
U1	7.1	0.0	3.6	0.0	89.2	100.00
A1	6.3	0.0	0.0	43.1	50.6	100.00
A2	11.2	0.0	4.2	0.0	84.6	100.00
A3	6.6	0.0	0.0	49.3	44.0	100.00
A4	7.4	0.0	0.0	17.6	75.0	100.00
A5	8.8	3.4	0.0	0.0	87.7	100.00
A6	8.7	3.7	0.0	37.0	50.6	100.00
A7	8.1	0.0	9.9	0.0	82.0	100.00
A14	9.8	0.0	3.4	0.0	86.8	100.00
A15	6.4	0.0	0.0	23.7	69.9	100.00
K-1	4.4	3.5	11.2	8.3	72.6	100.00
K-2	4.3	6.4	9.0	4.6	75.6	100.00
K-4	4.8	0.0	3.7	57.7	33.7	100.00
K-5	3.3	0.0	6.7	29.3	60.7	100.00
K-6	5.0	3.5	8.4	0.0	83.1	100.00
K-9	3.3	0.0	6.5	21.6	68.5	100.00
K-12	5.0	25.5	10.7	0.0	58.8	100.00
K-13	4.9	3.0	8.1	3.9	80.1	100.00
K-15	4.5	3.7	7.7	4.6	79.5	100.00
K-16	2.8	0.0	10.7	0.0	86.4	100.00
K-19	5.6	0.0	0.0	0.0	94.4	100.00
K-21	4.6	0.0	7.9	5.4	82.1	100.00
K-24	5.5	0.0	7.5	0.0	87.0	100.00
K-27	5.5	3.4	0.0	5.7	85.3	100.00
K-30	3.9	12.8	8.1	6.9	68.2	100.00
K-33	4.2	11.3	7.9	4.2	72.4	100.00
K-35	5.0	3.3	7.7	0.0	84.1	100.00
K-37	4.3	2.9	6.9	0.0	85.9	100.00
K-39	4.1	3.2	7.1	0.0	85.6	100.00
K-40	4.5	4.0	0.0	0.0	91.5	100.00
K-41	0.0	3.1	43.9	0.0	53.0	100.00

from 2.6 to 11.6 %. Dolomite appears in the lower parts of the section at a very low quantity and then is absent at some levels. However, it shows an increasing trend towards the upper part of the section where calcite is absent. The abundance of dolomite varies from a maximum of 66.3 % to a minimum of 3.4 %. Dolomite is found with calcite only at the bottom of the section. This trend was checked and confirmed by XRD and also by the staining test under the microscope. Feldspars, like calcite, are much more abundant at the bottom of the section and occur at lower values close to the upper levels. Their abundance ranges from 3.4 % to 11.2 % through the section. Total clay mineral amounts gathered from XRD diagrams are generally higher than 40 %. The minimum value for clay mineral abundance is 33.7 % and the maximum is 94.4 %.

The clay-fraction of the studied samples of Karahamzalı section reveals the presence of smectite, chlorite, kaolinite, illite and palygorskite in a decreasing order in the Karahamzalı section. Smectite, the dominant clay mineral found in the section is present in all samples including K-41 (the basaltic body). It was identified by the 12 Å–14 Å peaks which shift to 17 Å by ethylene glycol solvation. Mg-saturation and glycerol solvation techniques yield detailed information on the type of the swelling clay minerals, where the smectite peak at 14.2 Å remains stable at 14.2 Å–14.3 Å reflections (Küçükuysal 2011). This behaviour is typical of the beidellite type smectite minerals (Thorez 1976). This was also confirmed by Ca-saturation at relative humidity of 54 % and Ca-saturation with glycol solvation treatments. The smectite of this section has a 14.2 Å reflection at Ca-saturation at relative humidity of 54 % which shifts to 17 Å peak by Ca-saturation and glycol solvation. Smectite collapsed to 10.1 Å reflection by K-saturation and heating treatments (Küçükuysal 2011). Kaolinite and chlorite are the two clay minerals present in all samples except the basaltic rock (K-41) underlying the paleosols. Kaolinite and chlorite have some reflections overlapping each other. However, as Thorez (1976) stated, chlorites have strong d(001) at 14 Å and d(003) at 4.7 Å peaks, which do not occur in kaolinites. Also, heating to 550 °C for an hour causes dehydroxylation of the hydroxide sheet which is seen as an increase in the intensity of the d(001) reflection of chlorites (Moore & Reynolds 1989). Heating to 550 °C in K-saturated samples or in unsaturated samples causes the collapse of kaolinite where chlorite would still have the 14 Å and 7.3 Å reflections.

Illite is the easiest to differentiate from others. Its basal reflections are stable with all treatments and heatings. Therefore, 10 Å d(001) remains constant throughout the saturations. It is almost absent in the lower section samples but appeared with its 10 Å reflection in the upper section samples at low quantity. The other mineral present in the clay fraction of the samples is palygorskite. It is easily recognized with its 10.4 Å –10.5 Å reflection. This peak collapses to 10.1 Å by heating to 550 °C. To overcome the peak-wise confusion on the presence of palygorskite with illite, SEM studies were also carried out to reveal its fibrous morphology and particular interwoven crystal orientation (Fig. 4). The presence of palygorskite is indispensably valuable in paleoclimatic studies where it is accepted as proxy data for the reconstruction of the paleoclimate of the region in this study.

The peak intensities of the clay minerals in the Karahamzalı section were used to quantify the amounts of smectite, chlorite, kaolinite, illite and palygorskite. The method of Biscaye (1965) was followed during the calculation of the relative amounts of the clay minerals (Table 2). According to this method, 1, 1, 2, 0.5 and 1 are used as intensity factors for kaolinite (7 Å), chlorite (14 Å), illite (10 Å), smectite (17 Å) and palygorskite (10.4 Å), respectively. Smectite shows enrichments and depletions. Its highest content is almost 100 % at the bottom of the section but it shows depletion up the section reaching almost an abundance of 8.7 %. Kaolinite and illite, the detrital phases, plot almost the same trends on the diagrams. Kaolinite abundance ranges between 3.2 % and 25.6 %; similarly illite has 4.3 % to 38.9 % abundance through the section. Chlorite, the other detrital mineral found in the section, shows an opposite trend with respect to kaolinite and illite. Its lowest value is 11.1 %, whereas it is

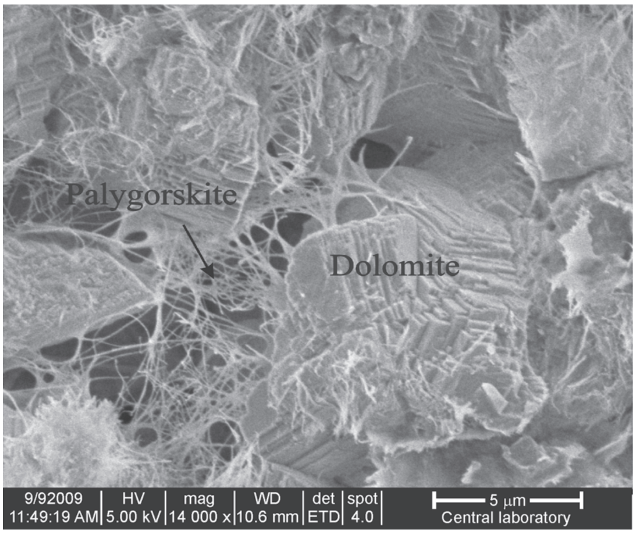

Fig. 4. SEM image on the bridge-like morphology of palygorskite fibres in paleosols of the Karahamzalı section.

Table 2: Semi-quantitative analysis of clay fraction of samples from the Karahamzalı section.

	Smectite	Chlorite	Palygorskite	Kaol.	Illite	SUM %
U-13	68.9	16.2	0.0	9.5	5.4	100.0
U-12	–	–	–	–	–	–
U-11	–	–	–	–	–	–
U-10	22.4	17.9	37.3	13.4	9.0	100.0
U-8	19.5	16.1	16.1	20.7	27.6	100.0
U-7	29.5	17.6	13.2	20.3	19.4	100.0
U-6S	44.5	21.1	0.0	16.7	17.6	100.0
U-6C	43.6	23.6	0.0	18.2	14.5	100.0
U-5	45.4	26.4	6.2	11.5	10.6	100.0
U-4	53.1	25.5	0.0	11.2	10.2	100.0
U-3	8.7	14.2	47.2	15.7	14.2	100.0
U-2	27.8	27.8	0.0	19.4	25.0	100.0
U-1	15.6	17.7	15.6	30.2	20.8	100.0
A-1	41.7	25.0	5.8	14.2	13.3	100.0
A-4	31.3	20.5	22.3	17.0	8.9	100.0
A-5	14.8	15.1	19.4	20.6	30.1	100.0
A-6	28.4	18.2	11.9	17.5	23.9	100.0
A-7	23.3	20.9	8.7	22.7	24.4	100.0
A-14	32.9	21.7	4.7	21.7	19.0	100.0
A-15	43.9	21.9	8.8	16.7	8.8	100.0
K-1	20.3	51.1	10.5	9.0	9.0	100.0
K-2	34.1	33.0	8.8	11.0	13.2	100.0
K-5	40.9	34.1	6.8	9.1	9.1	100.0
K-6	21.2	15.4	13.5	26.9	23.1	100.0
K-9	42.5	30.0	7.5	10.0	10.0	100.0
K-12	23.1	20.5	0.0	25.6	30.8	100.0
K-13	22.2	11.1	5.6	22.2	38.9	100.0
K-15	47.1	17.6	11.8	11.8	11.8	100.0
K-16	0.0	84.6	0.0	15.4	0.0	100.0
K-19	30.0	20.0	13.3	10.0	26.7	100.0
K-21	36.7	23.3	10.0	10.0	20.0	100.0
K-24	33.3	27.5	11.8	11.8	15.7	100.0
K-27	40.7	25.9	7.4	11.1	14.8	100.0
K-30	44.9	29.0	0.0	14.5	11.6	100.0
K-33	37.5	18.8	0.0	18.8	25.0	100.0
K-35	69.0	13.8	6.9	3.4	6.9	100.0
K-37	57.4	19.7	6.6	3.3	13.1	100.0
K-39	64.9	17.5	7.0	3.5	7.0	100.0
K-40	67.7	16.1	6.5	3.2	6.5	100.0
K-41	100.0	0.0	0.0	0.0	0.0	100.0

84.6 % at maximum in the section. Palygorskite plots exactly an opposite trend line to smectite and chlorite. The best line for palygorskite abundance through the section shows an increasing trend towards the top of the section. It starts with 4.7 % abundance and reaches a maximum of 47.2 %. The dolomite stochiometry study was done by Küçükuysal (2011) and the dolomites were evaluated as low to moderate for Ca-rich types and secondary dolomites.

Micromorphology

The cementing material of the paleosols is fine grained carbonate mineral, the size of which possibly suggests relatively rapid precipitation. The grains are formed from mineral and rock fragments. They have subangular to subrounded edges implying that the source of those clasts is not so far away from their provenance. The carbonate nodules are also common in the calcretes of the Karahamzalı section. The mineral and rock fragments, voids and dissolution channels are surrounded by carbonate minerals which are a typical feature of calcretes (Fig. 5A). Manganese dioxide coatings also rim some grains and also occur as dense compound infillings (Fig. 5B) and loose discontinuous clusters within the voids (Fig. 5C). Cracks and faunal passages in the calcretes are filled by coarse grained carbonate minerals. Carbonate nodules, as distinctive features of paleosols and their carbonates, and some voids are surrounded by carbonate minerals having distinct sharp and angular edges as dog-tooth cement. The presence of root fragments was also observed within the paleosols (Fig. 5D).

Calcretes developed within the reddish-brown coloured paleosols in the Karahamzalı section have a distinct similar colour to the paleosols as a primary feature which can easily be interpreted as being part of the soil profile. The arrangement of the peds within the lower horizons of the Karahamzalı succession integrates from a subangular blocky to prismatic structure. The peds are bound by angular and subrounded surfaces. Through the upper levels of the succession, the shapes of the peds change to subangular blocky and to granular, where primary peds are more or less similar in size, and secondary smaller ones indicate more advanced physical soil formation than the lower layers. In general, the microstructure of the paleosols within the Karahamzalı succession are subangular blocky to granular and prismatic (Fig. 5E). The peds of the paleosols (measure of the degree to which adjacent faces are moulds of each other) are also well accommodated in the lower levels of the succession, but vary from partial to unaccommodated towards the upper parts of the succession.

One of the important pedofeatures in paleosols of the Karahamzalı section are the clay coatings, clay skins or the so called clay cutans (Fig. 5F). The coatings are found as illuviated clay features in the paleosol matrix. Polysynthetic quartz grains, feldspar surfaces with weathering features, rock fragments of volcanic origin, cherts, clastic sedimentary rocks, basaltic and metamorphic rocks are observed as floating grains in thin sections. Other pedofeatures observed are the coatings and infills of MnO_2 along with carbonate minerals. Additionally, the secondary carbonate linings are also accepted as important features of paleosols and their carbonates. The Karahamzalı succession is a good example for paleosols and calcretes, both having secondary carbonate rims around floating grains, voids and carbonate nodules. This fabric feature indicates the presence of pedogenic formation in the calcretes of the Karahamzalı succession. The geometric relationship of the U-shaped voids within the calcretes of the Karahamzalı succession directly implies the evidence of the presence of past bioturbation. This is a prime phenomenon for classifying the calcretes of the study as beta calcretes according to Tucker (1991).

Geochemistry

The mineralogical and chemical compositions of the paleosols are strongly controlled by the geochemistry of the soil solution. Therefore, the geochemical characteristics of the paleosols and their carbonates can be employed as important proxies revealing the climatic history of the soil. The studies on paleosol geochemistry (Retallack 1997, 2001; Sheldon & Tabor 2009) stated that different proxies based on geochemical analyses can be used to infer the pedogenic processes revealing the effect of chemical weathering in paleosols (Table 3 in Küçükuysal et al. 2012). The whole rock geochemical analysis of the samples from the Karahamzalı section is already listed in Table 7.2 in Küçükuysal 2011 (p. 151). In this context, salinization should reflect the preferential removal of sodium relative to potassium in the surface horizons, where The Na_2O/K_2O ratio of salinization ranges from 0.1 to 0.41 for the Karahamzalı samples (Fig. 6). The increase towards the upper horizons is evidence of evaporation indicating a consequent water movement in the paleosols. Salinization for the arid-climatic conditions should be greater than 1, however, in this case, it reaches a maximum of almost 0.6 without passing a reference standard (Fig. 6). Calcification reflected in the ($CaO+MgO/Al_20_3$) ratio has a minimum value of 0.6 and maximum of 15.9. It is high in calcretes and low in paleosol levels throughout the section with increasing calcification values towards the surface (Fig. 6).

The other paramater is the clayeyness suggesting a clay accumulation rate varying from 0.14 to 0.22 which can be regarded as almost constant throughout the profile with a depletion trend towards the top of the section in calcrete horizons (Fig. 6). The plot of relative base loss vs. depth reflects the removal of mobile cations from the surface horizons and their accumulation at depth. Relative base loss values for the Karahamzalı section range from 0.06 to 1.28 documenting the medium to high weathering of the paleosols and the leaching of carbonates throughout the section (Fig. 6). Leaching values are consistent with the earlier studies in that it is high in paleosol levels and very low in calcrete levels. The values of leaching for the Karahamzalı Section range from 0.43 to 2.92 (Fig. 6). Normally leaching values are expected to be greater than 2 in well-drained soils with Na and K concentrations well correlated with the leaching trends. This is the case for the Karahamzalı section since it is seasonally well-drained; the leaching values in paleosols are high. In arid conditions, the leaching values decrease leading to the precipitation of calcium and magnesium carbonates.

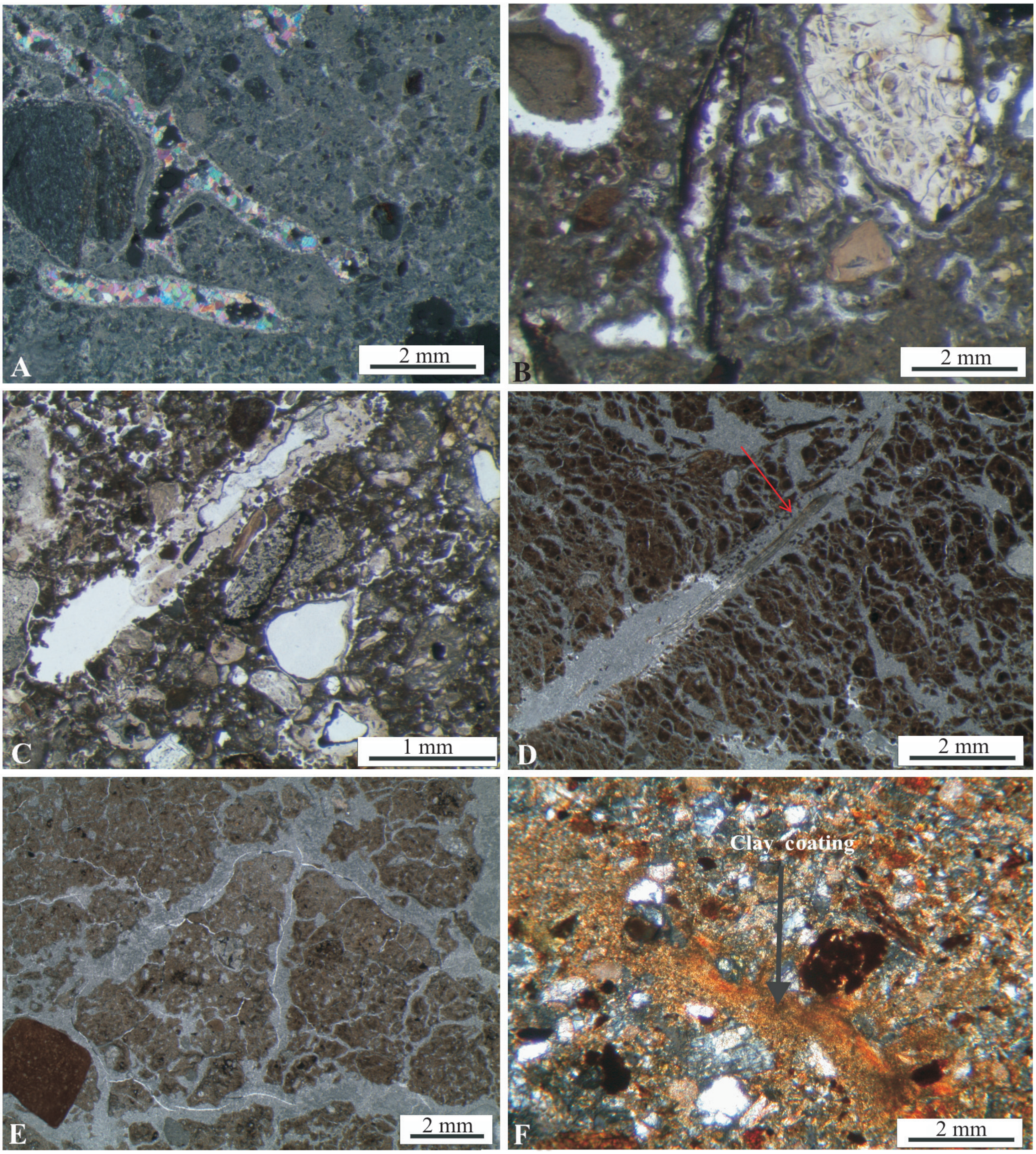

Fig. 5. Photomicrographs: **A** — of two almost parallel void spaces surrounding a rock fragment and filled with sparry carbonate including MnO_2 clusters; **B** — dense and continuous infilling of MnO_2 within a void space and around a feldspar fragment within a calcrete sample of the Karahamzalı succession; **C** — clusters of broken/beaded MnO_2 coatings within a void space in a calcrete sample from the Karahamzalı succession with probable organic infill; **D** — plant parts and faecal excrements within the U-11 paleosol sample of Karahamzalı succession; **E** — Subangular blocky microstructure and well accommodated ped structure of the paleosols within the Karahamzalı succession; **F** — pedofeature of clay coatings.

To measure the degree of chemical weathering, a value can be obtained by calculating the chemical index of alteration (CIA) of the section in terms given by Nesbitt & Young (1982) using molecular proportions of some elements. The higher the value, the more intense is the weathering. The CIA values of paleosols range from 73.42 to 82.97 for the Karahamzalı section (Fig. 6). This suggests that the paleosols were affected intensively by weathering. Another

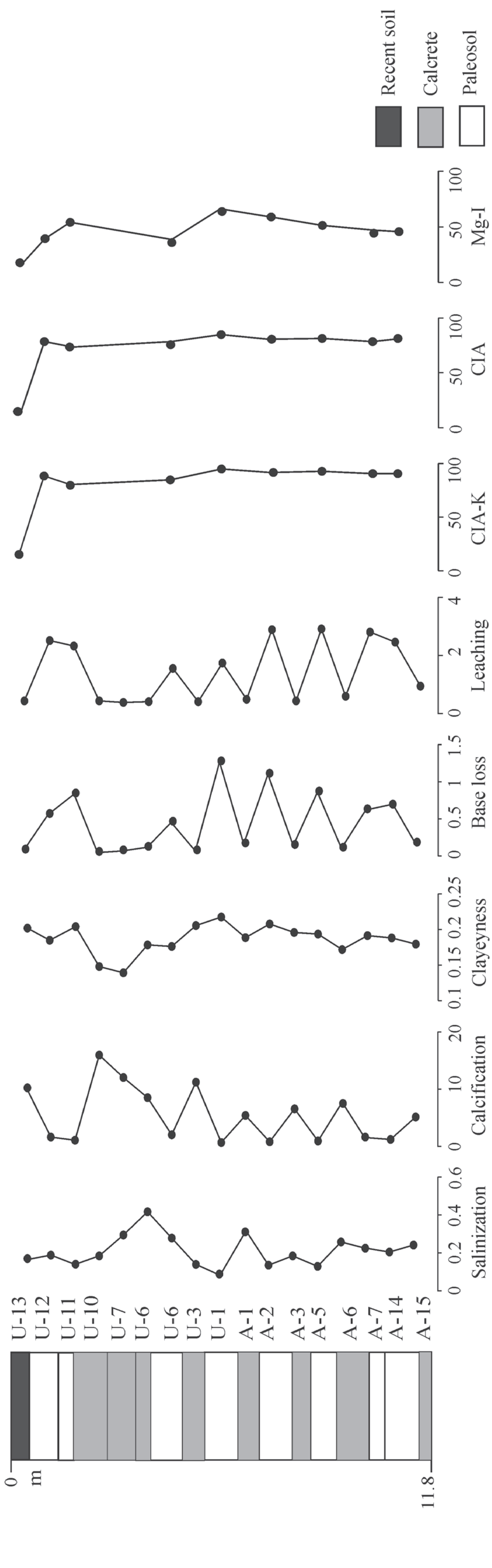

Fig. 6. Molecular weathering ratios calculated and chemical index of alteration values of the Karahamzalı paleosols and carbonates.

measure for the chemical index of alteration is CIA-K which omits the K addition. This value ranges from 80.70 to 92.6 for soils which are very similar to CIA values (Fig. 6). Considering 50 as CIA and CIA-K standard for paleosols, the studied paleosol samples are greater than 50, implying a high degree of chemical weathering for paleosols. The Mg index is also used to assess the weathering affect on paleosols and is calculated as 35 to 63.4 for paleosols, which are almost consistent with the CIA and CIA-K values (Fig. 6).

Weathering trends can be displayed on an Al_2O_3–$CaO+Na_2O$–K_2O (A-CN-K) triangular plot of Nesbitt & Young (1984, 1989). Rollinson (1993) summarized the trends on an A-CN-K triangular diagram as follows: Initial stages of weathering form a trend parallel to the CN-A side of the diagram, whereas advanced weathering shows a marked loss in K_2O as compositions move towards the Al_2O_3 apex. The trend follows mixing lines representing the removal of alkalis and Ca in solution during the breakdown of first plagioclase and then potassium feldspar and ferromagnesian silicates. Deviations from such trends can be used to infer chemical changes resulting from diagenesis or metasomatism (Nesbitt & Young 1984, 1989). The paleosols of the Karahamzalı section plot a trend line on the A-CN-K triangular diagram (Fig. 7). The paleosols show a weathering trend line slightly parallel to the CN-A side of the diagram with a small deviation towards the loss of K. This implies the very early stages of diagenesis.

Stable isotope geochemistry

Stable isotope results are measured relative to a standard, VSMOW or VPDB. They are expressed with delta notation (δ) in parts per thousand (‰ or per mil). The isotopic composition of carbonates in the Karahamzalı section exhibit a narrow range in $\delta^{13}C$ composition from −7.11 ‰ to −7.74 ‰ and a relatively narrower range in $\delta^{18}O$ composition from −3.97 ‰ to −4.91 ‰ (Table 3). Upward lower values in $\delta^{13}C$ were observed at the U10, U6C, A1, A6 and A15 levels, but $\delta^{13}C$ was enriched in the U7 and A3 levels of calcretes of the Karahamzalı section. An almost parallel trend to $\delta^{13}C$ is observed in $\delta^{18}O$ composition through the section in that it

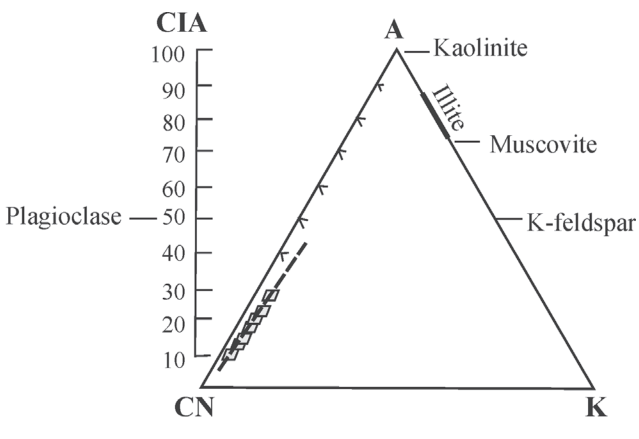

Fig. 7. Karahamzalı samples on the A-CN-K triangular plot of Nesbitt & Young (1984, 1989).

Table 3: $\delta^{13}C$ and $\delta^{18}O$ isotope compositions of the samples from the Karahamzalı section.

	$\delta^{13}C$	$\delta^{18}O$	$\delta^{18}O$
Sample	**VPDB**	**VSMOW**	**VPDB**
U-5	–7.4	26.4	–4.4
A-4	–7.7	26.2	–4.6
U-7	–7.3	26.2	–4.6
U-6c	–7.6	26.3	–4.4
A-6	–7.6	26.3	–4.5
U-2	–7.6	26.4	–4.4
A-15	–7.8	25.7	–5.0
A-1	–7.7	26.5	–4.2
A-3	–7.1	26.8	–3.9
U-10	–7.7	25.9	–4.9
U-13	–7.5	26.0	–4.7

shows upward depletions and enrichments at the same levels with $\delta^{13}C$ except U6. Therefore, it can be mentioned that a good covariance is observed between $\delta^{13}C$ and $\delta^{18}O$ values of carbonates in the Karahamzalı section. The ranges of stable isotope values are typical of a meteoric vadose environment (James & Choquette 1990). The measured carbon isotope compositions of calcretes are close to the isotope values typical for the soil carbonate formed from organic CO_2 produced predominantly by C4 vegetation cover and support a pedogenic or shallow groundwater origin (Bajnoczi et al. 2006). The $\delta^{18}O$ values are also in the range of normal continental soil carbonate (Cerling 1984) and do not indicate precipitation from evolved groundwater. The $\delta^{18}O$ enrichment at the top of the section is well-correlated with the water evaporation process. The increase in $\delta^{13}C$ and $\delta^{18}O$ values of carbonates implies an increase in the temperature. Such an arid and warmer climate favour the increase in C4-vegetation flora together with greater input of atmospheric CO_2 into the profile and results in higher $\delta^{13}C_{carbonate}$ and $\delta^{18}O_{carbonate}$ (Cerling 1984; Alam et al. 1997; Andrews et al. 1998).

Evaluation of the proxies

Palygorskite has a general increasing pattern up to the section indicating increasing aridity (Fig. 8). At the same time, smectite shows a general decreasing pattern towards the top (Fig. 8). Dolomite, similar to palygorskite has a general increasing trend towards the top of the section, becoming abundant in the calcrete levels (Fig. 8). As smectite decreases in amount, palygorskite becomes enriched, possibly suggesting the smectite weathering as one of the sources of Mg for the palygorskite formation (Fig. 8). It is also somewhat true for dolomite (for the formation of dolomite, Mg is also needed) abundance that where the amount of smectite decreases, dolomite becomes abundant. Therefore, this trend also implies that smectite may also be one of the Mg sources for dolomite formation. In addition, scanning electron images of the palygorskites in the Karahamzalı section show that palygorskites cover the dolomites and form bridge-like structures (Fig. 4). This also confirms the formation of palygorskite from the soil solution enriched in Mg. Dolomites are generally found within the pore spaces with rhombohedral forms and covered with palygorskites implying that they were formed before palygorskite formations. It is possible to accept that the secondary minerals, palygorskite and dolomite were formed during the process of paleosol development by modification due to the compaction-derived diagenesis. Under normal pedogenic circumcitances, presence of such mineral may be utilized for the paleoclimatic reconstructions. Their relative abundances through the section may well indicate the climatic conditions during the soil development (Fig. 8).

Molecular weathering ratios of the paleosols and calcretes of the Karahamzalı section display different trends. These values fluctuate between paleosol and calcrete levels. Calcification and salinization are very similar in both and increase towards the upper sections. This implies increasing aridity with increasing temperature (Fig. 8). The chemical indexes of

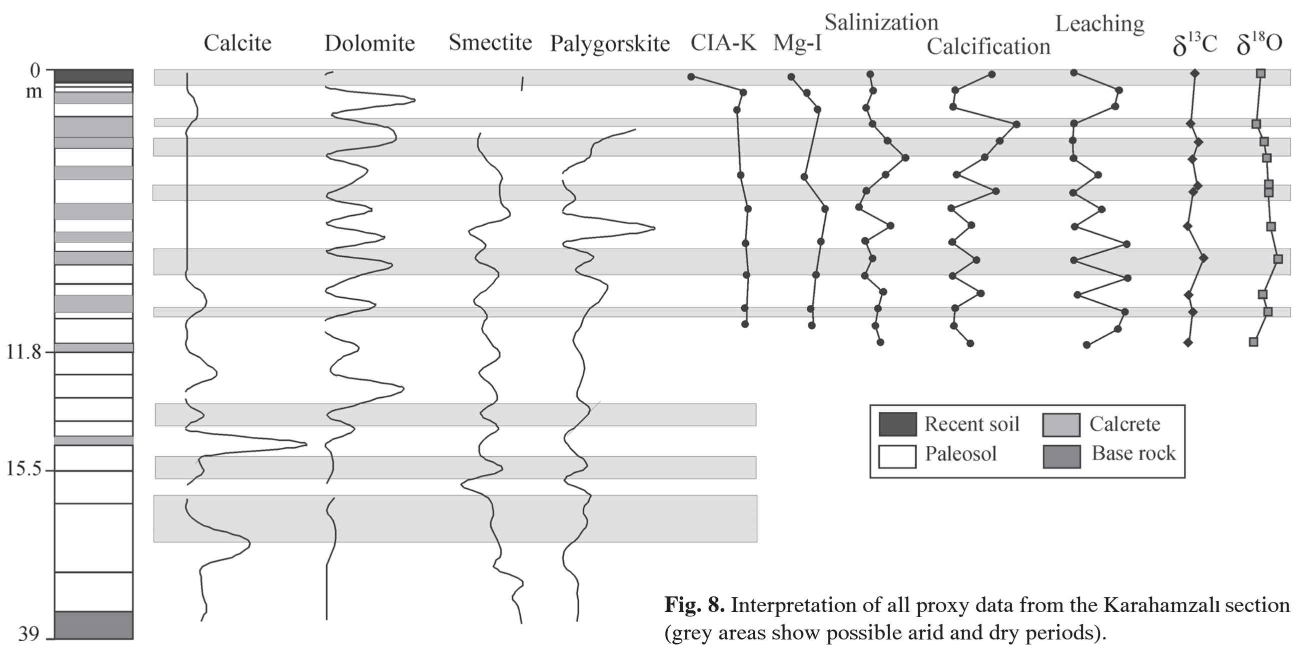

Fig. 8. Interpretation of all proxy data from the Karahamzalı section (grey areas show possible arid and dry periods).

the alteration values of CIA-K are parallel to the alteration values of MgI. These values are high within the paleosol levels (Fig. 8). The highest values are greater than 50 which suggest the occurrence of a medium degree of weathering within the paleosols. The alteration values only show a decreasing trend at the top where recent soil is occupied (Fig. 8).

As Nesbitt & Young (1982) stated, chemical weathering is mainly controlled by moisture and temperature. The stable patterns of the element records of the Karahamzalı section indicate that a wet climate occurs in enhanced chemical weathering conditions during the pluvial periods, while a dry climate favours the formation of calcretes during interpluvials.

There is a positive correlation between $\delta^{18}O$ and $\delta^{13}C$ values of the paleosol carbonates which indicates closed environmental conditions (Fig. 8). These are also consistent with the constant provenance values of trace elements (Küçükuysal 2011) suggesting that there was no additional influx to the system during the deposition of the units in the Karahamzalı section. This leads to the development of sedimentary units with similar characteristics.

Different generations of carbonates with almost stable geochemical composition conditions were detected. The $\delta^{13}C$ values ranging around −7 ‰ indicate high input of $\delta^{13}C$ from lower soil respiration rates in dry seasons which typically correlates with the vegetation cover dominated by C4 plants and are accompanied by higher $\delta^{18}C$ values due to evaporation (Driese & Mora 1993).

It is clear in Figure 8 that if all proxies are compared, it is possible to conclude that the dry and wet periods alternate through the paleosol sequence, in which dry periods favour an increase in palygorskite and dolomite with higher isotope signatures, while wet periods favour an increase in smectite and decrease in molecular weathering ratios (Fig. 8). It is clear that the studied section shows an alternation from wet to dry conditions led by pluvials and interpluvials favouring the formation of red-brownish coloured paleosols and their carbonates. All this evidence points to the view that the formation of carbonates may have occurred under early diagenetic conditions during the shallow burial of the paleosols under arid and dry climatic conditions.

Brief summary of the Eastern Mediterranean Quaternary climatic archives

Turkish continental records of Quaternary climates are well listed in Nicoll & Küçükuysal (2012). Lake Van (Wick et al. 2003; Litt el al. 2009), Eski Acıgöl (Woldring & Bottema 2003; Roberts et al. 2011) and Konya Basin (Fontugne et al. 1999; Roberts et al. 1999) have climatic archives through the Quaternary while Lake Abant (Bottema et al. 1993–1994; Roberts et al. 2011), Gölhisar (Eastwood et al. 1999) and Sofular Cave (Göktürk et al. 2011) only passed the Holocene. The Eastern Mediterranean continental climate archives like Lake Mirabad (Stevens et al. 2006; Roberts et al. 2011), Qunf Cave (Fleitmann et al. 2007), Lake Lisan (Bartov et al. 2003; Kolodny et al. 2005), Jeita Cave (Verheyden et al. 2002; Göktürk et al. 2011), Soreq Cave (Bar-Matthews et al. 2003; Göktürk et al. 2011) and Lake Zeribar (Stevens et al. 2001; Wasylikowa et al. 2006) also passed through the Quaternary.

Like the isotopic covariance in the central and southern Turkey with eastern Mediterranean Carbonates, this property was also identified in the carbonates of southern Europe (Sorbas Basin, Karlich Rhine Valley, Elsterian Loess, Holsteinian Paleosol, Carbonates from Crete) (Candy et al. 2012). The studied calcretes have the stable isotopic compositions implying the formation controlled by the same environmental factors. As Candy et al. 2012 suggested for the Mediterranean carbonates, aridity appears to be the major control on both $\delta^{18}O$ and $\delta^{13}C$ values in the studied soil carbonates with evaporation and CO_2 degassing. This is confirmed with the low leaching values during the dry seasons favouring the formation of carbonate rich soil and/or calcretes.

Conclusion

The pedofeatures determined in the alluvial deposits of the studied section contribute to understanding the development of the paleosols and the relevant formation of the calcretes in the Karahamzalı section. This study reveals that there is a consistency between the isotope values, the mineralogical compositions, the geochemical and micromorphological characteristics of the paleosols and calcretes throughout the Karahamzalı section.

The microstructural units of the paleosols and calcretes point the formation in the vadose zone of the depositional environment, where the semi-mature dolomite bearing calcretes with biological activity are also present. Considering the age of the paleosols as Late Pliocene–Pleistocene, it is possible to conclude that the calcretes in Karahamzalı section formed almost at the same time as the calcretes in Bala, Central Anatolia (Küçükuysal et al. 2012). Therefore, the climates of the Late Pliocene–Pleistocene in the Karahamzalı section favour the formation of the paleosols and their calcretes during the fluctuations from arid and dry to humid and wet conditions with mainly C4 vegetation.

Acknowledgments: This study is a part of a PhD Thesis completed by the author, which was financially supported by TÜBİTAK under the Project of 106Y172. The author is grateful to Prof. Dr. Fred J. Longstsaffe from the University of Western Ontario, Canada, for his help during mineralogical and stable isotope analysis of the samples And last but not the least Prof. Dr. Asuman Türkmenoğlu has devoted much effort on all occasions as the adviser of the thesis. The reviewers of this manuscript are kindly acknowledged for their constructive comments.

References

Akçay A.E., Dönmez M., Kara H., Yergök A.F. & Esentürk K. 2008: Geological Maps of Turkey in 1 : 100,000 scale, Kırşehir J-30 Sheet. [1 : 100,000 ölçekli Türkiye Jeoloji Haritaları Kırşehir J-30 Paftası.] *MTA Publ.,* Ankara, No. 91.

Alam M.S., Keppens E. & Paepe R. 1997: The use of oxygen and carbon isotope composition of pedogenic carbonates from Pleistocene palaeosols in NW Bangladesh, as palaeoclimatic indicators. *Quarter. Sci. Rev.* 16, 161–168.

Andrews J.A., Singhvi A.K., Kailath A.J., Kuhn R., Dennis P.F., Tandon S.K. & Dhir S.P. 1998: Do stable isotope data from calcrete record Late Pleistocene monsoonal climate variation in the Thar Desert of India? *Quat. Res.* 50, 240–251.

Atabey E., Atabey N. & Kara H. 1998: Sedimentology of caliche (calcrete) occurrences of the Kırşehir region. *Bull. Miner. Res. Explor.* 120, 69–80.

Atalay I. 1996: Palaeosols as indicators of the climatic changes during Quaternary period in S Anatolia. *J. Arid Environments* 32, 23–35.

Bajnóczi B., Horváth Z., Demény A. & Mindszenty A. 2006: Stable isotope geochemistry of calcrete nodules and septarian concretions in a Quaternary 'red clay' paleovertisol from Hungary. *Isotopes in Environmental and Health Studies* 42, 335–350.

Bar-Matthews M., Ayalon A., Gilmour M., Matthews A. & Hawkesworth C.J. 2003: Sea-land isotopic relationships from planktonic foraminifera and speleothems in the Eastern Mediterranean region and their implication for palaeorainfall during interglacial intervals. *Geochim. Cosmochim. Acta* 67, 3181–3199.

Bartov Y., Goldstein S.L., Stein M. & Enzel Y. 2003: Catastrophic arid episodes in the Eastern Mediterranean linked with the North Atlantic Heinrich events. *Geology* 31, 439–442.

Biscaye P.E. 1965: Mineralogy and sedimentation of recent deep sea clay in the Atlantic Ocean and adjacent seas and oceans. *Geol. Soc. Amer. Bull.* 76, 803–832.

Bottema S., Woldring H. & Aytuğ B. 1993–1994: Late Quaternary vegetation history of northern Turkey. *Palaeohistoria* 35, 36, 13–72.

Brindley G.W. 1980: Quantitative X-ray analyses of clays. In: Brindley G.W. & Brown G. (Eds.): Crystal structures of clay minerals and their X-ray identification. *Miner. Soc., Monograph* 5, 411–438.

Buol S.W., Hole F.D., McCracken R.J. & Southard R.J. 1997: Soil genesis and classification. *Iowa State University Press*, *Mes-Ames*, IA, 1–527.

Candy I., Adamson K., Gallant C.E., Whitfield E. & Rope R. 2012: Oxygen and carbon isotopic composition of Quaternary meteoric carbonates from western and southern Europe: their role in palaeoenvironmental reconstruction. *Palaeogeogr. Palaeoclimatol. Palaeoecol.* 326–328, 1–11.

Cerling T.E. 1984: The stable isotope composition of modern soil carbonate and its relationship to climate. *Earth Planet. Sci. Lett.* 71, 229–240.

Driese S.G. & Mora C.I. 1993: Physico-chemical environment of pedogenic carbonate formation in Devonian vertic palaeosols, central Appalachians, USA. *Sedimentology* 40, 199–216.

Eastwood W.J., Roberts N., Lamb H.F. & Tibby J.C. 1999: Holocene environmental change in southwest Turkey: A palaeoecological record of lake and catchment-related changes. *Quarter. Sci. Rev.* 18, 671–696.

Eren M. 2011: Stable isotope geochemistry of Quaternary calcretes in the Mersin area, southern Turkey — A comparison and implications for their origin. *Chemie der Erde* 71, 31–37.

Eren M., Kadir S., Hatipoğlu Z. & Gül M. 2008: Quaternary calcrete development in the Mersin area, southern Turkey. *Turkish J. Earth Sci*. 17, 763–784.

Fitzpatrick E.A. 1993: Soil microscopy and micromorphology. *John Wiley and Sons Ltd*., 1–304.

Fleitmann D., Burns S.J., Mangini A., Mudelsee M., Kramers J. & Villa I. 2007: Holocene ITCZ and Indian monsoon dynamics recorded in stalagmites from Oman and Yemen (Socotra). *Quarter. Sci. Rev.* 26, 170–188.

Fontugne M., Kuzucuoğlu C., Karabiyikoğlu M., Hatté C. & Pastre J.F. 1999: From Pleniglacial to Holocene: a ^{14}C chronostratigraphy of environmental changes in the Konya Plain, Turkey. *Quarter. Sci. Rev.* 18, 573–591.

Goudie A.S. 1973: Duricrusts in tropical landscapes. *Clarendon Press*, Oxford, 1–174.

Goudie A.S. 1983: Calcrete. In: Goudie A.S. & Pye K. (Eds.): Chemical sediments and geomorphology. *Academic Press*, London, 93–131.

Göktürk O.M., Fleitmann D., Badertsscher S., Cheng H., Edwards R.L., Leuenberger M., Fankhauser A., Tüysüz O. & Kramers J. 2011: Climate on the southern Black Sea coast during the Holocene: implications from the Sofular Cave record. *Quarter. Sci. Rev.* 30, 2433–2445.

Gündoğdu M.N. 1982: Geological, mineralogical and geochemical investigation of the Bigadiç Neogene volcano-sedimentary sedimentary basin. *PhD Thesis*, Hacettepe University, Ankara, Turkey, 1–368 (unpublished).

Gürel A. & Kadir S. 2006: Geology, mineralogy and origin of clay minerals of the Pliocene Fluvial-Lacustrine deposits in the Cappadocian Volcanic Province, Central Anatolia, Turkey. *Clays and Clay Miner.* 54, 555–570.

Jackson M.L. 1979: Soil chemical anaylsis-advanced course. 2nd edition. *Published by the author*, Madison, Wisconsin, U.S.A., 1–895.

James N.P. 1972: Holocene and Pleistocene calcareous crust (caliche) profiles: Criteria for subaerial exposure. *J. Sed. Petrology* 42, 817–836.

James N.P. & Choquette P.W. 1990: Limestones — the sea floor diagenetic environment. In: Mcireath A. & Morrow D.W. (Eds.): Diagenesis. *Geosci. Canada Report Ser*. 4, 13–34.

Kapur S., Çavuşgil V.S. & Fitzpatrick E.A. 1987: Soil-calcrete (caliche) relationship on a Quaternary surface of the Çukurova Region, Adana (Turkey). In: Federoff N., Bresson L.M. & Courty M.A. (Eds.): Soil micromorphology. *Assoc. Francaise pour L'Etude du sol*, Paris, 597–603.

Kapur S., Yaman S., Gökçen S.L. & Yetiş C. 1993: Soil stratigraphy and Quaternary caliche in the Misis area of the Adana Basin, southern Turkey. *Catena* 20, 431–445.

Kapur S., Çavuşçugil V., Şenol M., Gürel N. & Fitzpatrick E.A. 1990: Geomorphology and pedogenetic evolution of Quaternary calcretes in the northern Adana Basin of southern Turkey. *Z. Geomorphology*, N.F. 34, 1, 49–59.

Kapur S., Saydam C., Akça E., Çavuşgil V.S., Karaman C., Atalay I. & Özsoy T. 2000: Carbonate pools in soil of the Mediterranean: a case study from Anatolia. In: Lal R., Kımble J.M., Eswaran H. & Stewart B.A. (Eds.): Global climate change and pedogenic carbonates. *Lewis Publishers*, Boca Raton, Florida, 187–212.

Kolodny Y., Stein M. & Machlus M. 2005: Sea-rain-lake relation in the Last Glacial East Mediterranean revealed by $\delta^{18}O$–$\delta^{13}C$ Lake Lisan aragonites. *Geochim. Cosmochim. Acta* 69, 4045–4060.

Kraus M.J. 1999: Paleosols in clastic sedimentary rocks: their geologic significance. *Earth Sci. Rev*. 47, 41–70.

Küçükuysal C. 2011: Palaeoclimatological approach to Plio-Quaternary paleosol-calcrete sequences in Bala and Gölbaşı (Ankara) by using mineralogical and geochemical proxies. *METU PhD Thesis*, Middle East Technical University, Ankara, Turkey, 1–246.

Küçükuysal C., Türkmenoğlu A.G. & Kapur S. 2013: Multi-proxy evidence of Mid-Pleistocene dry climates observed in calcretes in Central Turkey. *Turkish J. Earth Sci*., 469–483. Doi: 10.3906/yer-1201-5

Küçükuysal C., Engin B., Türkmenoğlu A.G. & Aydaş C. 2011: ESR dating of calcrete nodules from Bala, Ankara (Turkey): Preliminary results. *Applied Radiation and Isotopes* 69, 492–499.

Litt T., Krastel S., Sturm M., Kipfer R., Örçen S., Heumann G., Franz S.O., Ülgen U.B. & Niessen F. 2009: "PALAEOVAN" International Continental Scientific Drilling Program, (ICDP):

Results of a recent site survey and perspectives. *Quat. Sci. Rev.* 28, 1555–1567.

Maynard J.B. 1992: Chemistry of modern soils as a guide to interpreting precambrian paleosols. *J. Geol.* 100, 279–289.

Moore D.M. & Reynolds J.R. 1989: X-ray diffraction and the identification and analysis of clay minerals. *Oxford University Press*, Oxford, 1–332.

Morozova T.D. 1995: Identification of paleosol types and their applicability for paleoclimatic reconstruction. *GeoJournal* 36, 2–3, 199–205.

Nesbitt H.W. & Young G.M. 1982: Early Proterozoic climates and plate motions inferred from major element chemistry of lutites. *Nature* 299, 715–717.

Nesbitt H.W. & Young G.M. 1984: Prediction of some weathering trends of plutonic and volcanic rocks based thermodynamic and kinetic considerations. *Geochim. Cosmochim. Acta* 48, 1523–1534.

Nesbitt H.W. & Young G.M. 1989: Formation and diagenesis of weathering profiles. *J. Geol.* 97, 129–147.

Nicoll K. & Küçükuysal C. 2013: Emerging multi-proxy records of Late Quaternary Palaeoclimate dynamics in Turkey and the surrounding region. *Turkish J. Earth Sci.* 22, 126–142.

Özer A.M., Wieser A., Göksu H.Y., Müller P., Regulla D.F. & Erol O. 1989: ESR and TL age determination of caliche nodules. *Int. J. Radiation Applications and Instrument*; Part A — *Applied Radiation and Isotopes* 40, 1159–1989.

Retallack G.J. 1997: A colour guide to paleosols. *Wiley*, Chichester, 1–175.

Retallack G.J. 2001: Soils of the past. *Blackwell*, Oxford, 1–600.

Roberts C.N., Eastwood W.J., Kuzucuoğlu C., Fiorentino G. & Caracuta V. 2011: Climatic, vegetation and cultural change in the eastern Mediterranean during the mid-Holocene environmental transition. *The Holocene* 21, 147–162.

Roberts N., Black S., Boyer P., Eastwood W.J., Griffiths H.I., Lamb H.F., Leng M.J., Parish R., Reed J.M., Twigg D. & Yigitbasuiglu H. 1999: Chronology and stratigraphy of late Quaternary sediments in the Konya basin, Turkey: results from the KOPAL project. *Quat. Sci. Rev.* 18, 611–630.

Sheldon N.D. & Tabor N.J. 2009: Quantitative paleoenvironmental and paleoclimatic reconstruction using paleosols. *Earth Sci. Rev.* 95, 1–52.

Stevens L.R., Wright Jr. H.E. & Ito E. 2001: Proposed changes in seasonality of climate during the Late-glacial and Holocene at Lake Zeribar, Iran. *The Holocene* 11, 747–756.

Stevens L.R., Ito E., Schwalb A. & Wright Jr. H.E. 2006: Timing of atmospheric precipitation in the Zagros Mountains inferred from a multi-proxy record from Lake Mirabad, Iran. *Quat. Res.* 66, 494–500.

Tabor N.J. 2002: Paleoclimate isotopic proxies derived from Paleozoic, Mesozoic, Cenozoic Paleosols and modern soils. *University of California, PhD Thesis*, Davis, California, 1–213.

Thorez J. 1976: Practical identification of clay minerals. *Lelotte*, Dison, Belgium, 1–89.

Tucker M.E. 1991: Sedimentary petrology: An introduction to the origin of sedimentary rocks. *Blackwell Science*, Oxford, viii+260.

Tucker M. 1988: Techniques in sedimentology. *Blackwell Scientific Publications*, Oxford, 1–394.

Verheyden S., Nader F., Cheng H., Edwards L. & Swennen R. 2008: Palaeoclimate reconstruction in the Levant region from the geochemistry of a Holocene stalagmite from the Jeita cave, Lebanon. *Quat. Res.* 70, 368–381.

Wasylikowa K., Witkowski A., Walanus A., Hutorowicz A., Alexandrowicz S.W. & Langer J.L. 2006: Palaeolimnology of Lake Zeribar, Iran, and its climatic implications. *Quat. Res.* 66, 477–493.

Wick L., Lemcke G. & Sturm M. 2003: Evidence of late glacial and Holocene climatic change and human impact in eastern Anatolia: high-resolution pollen, charcoal, isotopic and geochemical records from the laminated sediments of Lake Van, Turkey. *The Holocene* 13, 665–675.

Woronick R.W. & Land L.S. 1985: Late burial diagenesis, Lower Cretaceous Pearsall and Lower Glenn Rose Formations, South Texas. *Soc. Econ. Paleont. Mineral., Spec. Publ.* 36, 265–275.

Wright V.P. & Tucker M.E. 1991: Calcretes. *Blackwell Scientific Publications*, Oxford, 1–351.